Evolutionary Migration of a Post-Translationally Modified Active-Site Residue in the Proton-Pumping Heme-Copper Oxygen Reductases†

James Hemp,[‡,§,||] Dana E. Robinson,[‡,||] Krithika B. Ganesan,[§] Todd J. Martinez,[‡] Neil L. Kelleher,[‡] and Robert B. Gennis*,[⊥]

Department of Chemistry, University of Illinois, Urbana, Illinois 61801, Center for Biophysics and Computational Biology, University of Illinois, Urbana, Illinois 61801, and Department of Biochemistry, University of Illinois, 600 South Mathews Avenue, Urbana, Illinois 61801

Received September 28, 2006; Revised Manuscript Received November 2, 2006

ABSTRACT: In the respiratory chains of aerobic organisms, oxygen reductase members of the heme-copper superfamily couple the reduction of O_2 to proton pumping, generating an electrochemical gradient. There are three distinct families of heme-copper oxygen reductases: A, B, and C types. The A- and B-type oxygen reductases have an active-site tyrosine that forms a unique cross-linked histidine−tyrosine cofactor. In the C-type oxygen reductases (also called cbb_3 oxidases), an analogous active-site tyrosine has recently been predicted by molecular modeling to be located within a different transmembrane helix in comparison to the A- and B-type oxygen reductases. In this work, Fourier-transform mass spectrometry is used to show that the predicted tyrosine forms a histidine−tyrosine cross-linked cofactor in the active site of the C-type oxygen reductases. This is the first known example of the evolutionary migration of a post-translationally modified active-site residue. It also verifies the presence of a unique cofactor in all three families of proton-pumping respiratory oxidases, demonstrating that these enzymes likely share a common reaction mechanism and that the histidine−tyrosine cofactor may be a required component for proton pumping.

Aerobic respiration plays a fundamental role in Earth's biogeochemical oxygen cycle. It has been estimated that ∼75% of the O_2 produced by oxygenic photosynthesis is reduced to water via this enzymatically catalyzed process, tightly coupling two of the most widespread metabolisms on earth. Aerobic respiration is also the most exergonic metabolism known and appears to be a requirement for multicellular life. Respiration is performed by a series of integral membrane protein complexes that form electron transfer chains, found within the inner mitochondrial membrane of aerobic eukaryotes and the cytoplasmic membrane of many prokaryotic organisms (*1*, *2*). Mitochondria have a linear electron transfer chain terminating with cytochrome *c* oxidase, a proton-pumping oxygen reductase which reduces O_2 to water. Prokaryotes have more complicated electron transfer chains with branches leading to different terminal electron acceptors (e.g., fumarate, nitrate, Fe^{3+}, O_2), allowing for metabolic flexibility when different environments are encountered.

Most aerobic prokaryotes utilize respiratory oxidases (i.e., oxygen reductases) that are members of the heme-copper superfamily, which is structurally and catalytically diverse, containing both oxygen reductases and nitric oxide reductases. The mitochondrial cytochrome *c* oxidase is also a member of the heme-copper superfamily. Heme-copper oxygen reductases catalyze the reduction of O_2 to water with the concomitant electrogenic translocation of protons across the membrane, contributing to the generation of a proton electrochemical gradient that can be coupled to energy-requiring cellular processes (*1*, *2*). The oxygen reductases are all multisubunit protein complexes that span the membrane bilayer. They are classified as A-, B-, or C-type oxygen reductases, on the basis of genomic, phylogenetic, and structural analyses (*1*). All three oxygen reductase families have been shown to pump protons coupled to the reduction of oxygen; however, they differ in biochemical properties such as reaction rate and oxygen affinity. Many prokaryotic genomes encode several heme-copper oxygen reductases which are differentially expressed depending on the environmental conditions.

Subunit I is the core protein in the enzyme complex and is the only subunit shared by all three families of the oxygen reductases. All of the amino acid residues and cofactors necessary for catalysis and proton pumping are within subunit I. The active site of the enzyme is a bimetallic center composed of a copper ion (Cu_B) and a high-spin heme, together ligated by four conserved histidines (three to Cu_B and one to the heme Fe). X-ray structures of members of the A- and B-type heme-copper oxygen reductases reveal a

† This work was supported by grants from the National Institutes of Health [GM 067193-04 (to N.L.K.) and HL 16101 (to R.B.G.)] and from the National Science Foundation [NSF-BES-04-03846 (to T.J.M.)].

* To whom correspondence should be addressed: Department of Biochemistry, University of Illinois, 600 S. Mathews Ave., Urbana, IL 61801. E-mail: r-gennis@uiuc.edu. Fax: (217) 244-3186. Telephone: (217) 333-9075.

‡ Department of Chemistry.

§ Center for Biophysics and Computational Biology.

|| These authors are equally responsible for the work that was performed.

⊥ Department of Biochemistry.

10.1021/bi062026u CCC: $33.50
Published on Web 12/19/2006

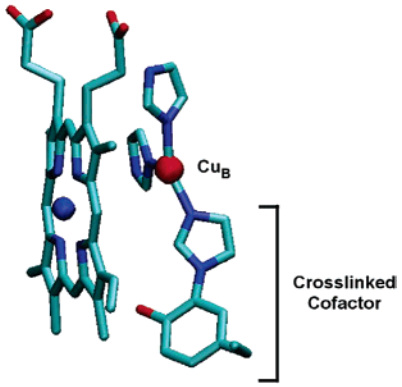

FIGURE 1: Structure of the active-site cofactor from *R. sphaeroides* A-type heme-copper oxygen reductase. The cofactor is formed by a covalent cross-link between the N_ϵ atom of a Cu_B histidine ligand and the C_ϵ atom of the active-site tyrosine and is present throughout the catalytic cycle. The farnesyl tail has been removed from the heme for clarity. This figure was generated using VMD (*45*).

unique cross-linked histidine−tyrosine cofactor in the active site between one of the Cu_B ligands and a tyrosine that is essential for enzyme function (*3*−*5*). This tyrosine is postulated to be oxidized to a tyrosyl radical during turnover and to donate a hydrogen atom to facilitate breaking of the O−O bond during catalysis (*6*−*8*). The cross-link has been verified by mass spectrometry in the B-type oxygen reductase from *Thermus thermophilus* (*9*). Figure 1 shows the structure of the cross-linked residues at the active site of the A-type oxygen reductases.

Sequence alignments have shown that the active-site tyrosine present in all of the A- and B-type oxygen reductases is absent in the C-type oxygen reductases. Recently, structural models of subunit I for the C-type oxygen reductases from *Vibrio cholerae* (*10*) and *Rhodobacter sphaeroides* (*11*) were built utilizing the X-ray structures of the A- and B-type oxygen reductases as templates. A surprising result was the prediction that a completely conserved tyrosine (Y255 in *V. cholerae*) from transmembrane helix VII in the C-type oxygen reductases occupies the same physical position in the active site as the tyrosine located in transmembrane helix VI of the A- and B-type oxygen reductases (*10*, *11*). It was also shown by modeling that it is geometrically feasible for a cross-link to be formed with the equivalent histidine ligand to Cu_B (H211 in *V. cholerae*). In this work, mass spectrometry was used to show that the predicted cross-link is indeed present in subunit I of the *V. cholerae* C-type oxygen reductase.

MATERIALS AND METHODS

All reagents are from Sigma (St. Louis, MO) unless otherwise noted.

Overexpression of C-Type Oxygen Reductase from V. cholerae. Protein was overexpressed and collected as previously reported (*10*). Briefly, *V. cholerae* cells were grown in LB medium (USB Corp.) with 100 μg/L ampicillin (Fisher Biotech) and 100 μg/L streptomycin at 37 °C. Gene expression was induced with 0.2% L-(+)-arabinose. The cells were lysed and centrifuged at 40 000 rpm to collect the membranes. Membrane proteins were solubilized by adding 0.5% dodecyl β-D-maltoside (Anatrace). Nonsolubilized membranes were removed by centrifugation at 40 000 rpm for 30 min.

Purification of Oxygen Reductase. To obtain a preparation sufficiently pure for mass spectrometry, the enzyme was first purified using immobilized metal affinity chromatography (IMAC) followed by weak anion exchange (WAX) on DEAE-Sepharose. IMAC was performed as previously reported (*10*), using a nickel affinity column (Qiagen, Valencia, CA) in a cold room (4 °C) at low pressure in 0.05% DDM and eluting the His-tagged protein using a stepped gradient of imidazole. WAX was performed using fast protein liquid chromatography (FPLC) [Amersham Biosciences (now GE Healthcare), Piscataway, NJ] in a cold room using 10 mM ammonium bicarbonate (pH 8.0) and 0.05% DDM as solvent A and 1 M ammonium bicarbonate and 0.05% DDM as solvent B. Samples were loaded at a percentage of solvent B that was approximately 10% below the expected elution concentration of solvent B for the protein complex as determined by test gradients. A 1 h gradient to 100% solvent B was then utilized, and fractions containing the purified protein were combined. After each chromatography step, the sample was concentrated using a centrifugal filter with a mass cutoff of 50 kDa (Millipore, Billerica, MA).

Trypsin Digestion of the Oxygen Reductase and Sample Preparation. Ten microliters of purified enzyme (approximately 25 mg/mL) was digested overnight with 20 μg of sequencing-grade trypsin (Bio-Rad, Hercules, CA) in a 90/10 100 mM ammonium bicarbonate (pH 8.0)/acetonitrile mixture at 37 °C. Immediately following trypsin digestion, 50 μL of the sample was applied to a gel filtration spin column with a 6 kDa mass cutoff (Micro Bio-Spin P6, Bio-Rad) to remove low-mass peptides. The spin column was equilibrated four times in 0.05% DDM prior to use. A methanol/chloroform precipitation (*12*, *13*) was then used to separate the remaining peptides from the detergent and soluble peptides. The resulting pellet was resuspended in 500 μL of 75% acetic acid and immediately subjected to analysis via mass spectrometry.

Mass Spectrometry. Samples were analyzed on a custom-built 8.5 T quadrupole Fourier-transform ion cyclotron resonance mass spectrometer (Q-FTICR MS) (*14*) using the MIDAS datastation (*15*). Introduction was performed using electrospray ionization (ESI) from a nanospray robot (Advion BioSciences, Ithaca, NY) at 1.2 kV with a backing gas pressure of 0.5 psi. Broadband scans were conducted to identify species of interest for fragmentation followed by quadrupole isolation (2 *m*/*z* window) and MS/MS using collisionally activated dissociation (CAD) in the external accumulation octopole (*16*, *17*). In these MS/MS experiments, several CAD acceleration voltages were used to generate a wider variety of fragment ions. The time for transfer into the ICR cell was also varied to compensate for time-of-flight effects.

Data Analysis. Data from the broadband and MS/MS experiments were processed using the THRASH algorithm (*18*) and analyzed with ProSightPTM [http://prosightptm-.scs.uiuc.edu (*19*)]. The presence of the cross-link required a separate fragmentation analysis of each of the two peptides, with the opposite peptide modeled as a single large post-translational modification. C-Terminal (B)- and N-terminal (Y)-type fragment ions (*20*) were matched at 20 ppm for the cross-linked peptide from the *V. cholerae* C-type oxygen reductase and 10 ppm for all other peptides.

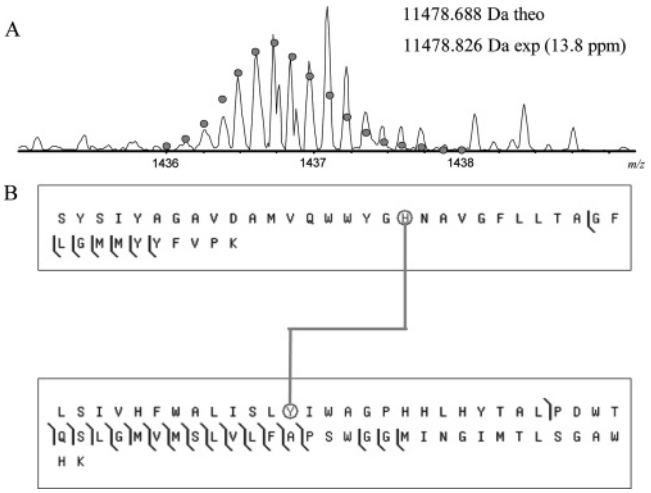

FIGURE 2: CAD fragmentation map for the cross-linked S193−K232 and L243−K304 peptides. (A) Mass spectrum of the cross-linked tryptic peptide. The circles show the theoretical isotope heights for a peptide of the given mass. (B) CAD MS/MS fragmentation results. The cross-linked histidine and tyrosine are circled. Spectra were processed using a modified version of the THRASH algorithm (*18*), and fragments were matched using ProSight PTM [http://prosightptm.scs.uiuc.edu (*46*)] with a match tolerance of 20 ppm.

RESULTS

Mass Spectrometry of a Tryptic Digest of a C-Type Oxygen Reductase. Mass spectrometry (MS) of a tryptic digest of subunit I from the *V. cholerae* C-type oxygen reductase was performed to discern the presence of the predicted cross-link. Analysis of the protein sequence predicted that if a cross-link was formed then complete trypsin digestion would result in a peptide containing residues S193−K232 cross-linked to residues L243−K304, but missing the region from residue Q233 to R242. This "H-shaped" tryptic peptide would not be present if the cross-link did not exist and was predicted to have a mass equal to that of the two individual peptides, subtracting 2 Da for the two protons lost during the formation of the cross-link. A peptide of this expected molecular mass (monoisotopic mass of 11 478.7 Da) was present in the mass spectrum of the trypsin digest. This cross-linked tryptic fragment was isolated and analyzed by tandem MS (MS/MS) using collisionally activated dissociation (CAD) fragmentation. Figure 2 shows the MS/MS fragment map of the cross-linked peptide. Multiple N- and C-terminal fragment ions were detected from the peptides on either end of the cross-link, demonstrating the existence of a cross-link between the two. In addition to the MS/MS fragment ions containing the cross-linked peptide, several of the MS/MS fragments spanned cross-linked residue Y255 but did not include the cross-link (Figure 3).

Presence of the Non-Cross-Linked Protein in the Digest. The trypsin digest also contained non-cross-linked S193−K232 and L243−K304 peptides, and detailed MS/MS fragmentation confirmed their identity (Figures 4 and 5). It is unclear whether the His−Tyr cross-link is normally absent in a portion of the population of the protein or if the non-cross-linked species is an artifact of the recombinant protein expression or sample preparation. To address the lability of the cross-link, the same protocol was used to investigate the cross-link in the A-type oxygen reductase from *Rhodobacter sphaeroides*. In the A-type oxygen reductases, the cross-link

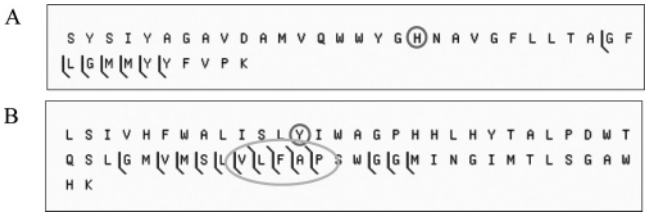

FIGURE 3: CAD fragmentation of the cross-linked tryptic peptide from the C-type oxygen reductase assuming the absence of the cross-link. The CAD fragmentation data set used to generate Figure 2 was also analyzed as if the cross-link were not present. (A) Matches for the tryptic S193−K232 and (B) for L243−K304 peptides. The histidine and tyrosine normally involved in the cross-link are circled. The oval highlights several fragments that were found to span the cross-linked residue but do not include the mass of the opposite cross-linked peptide.

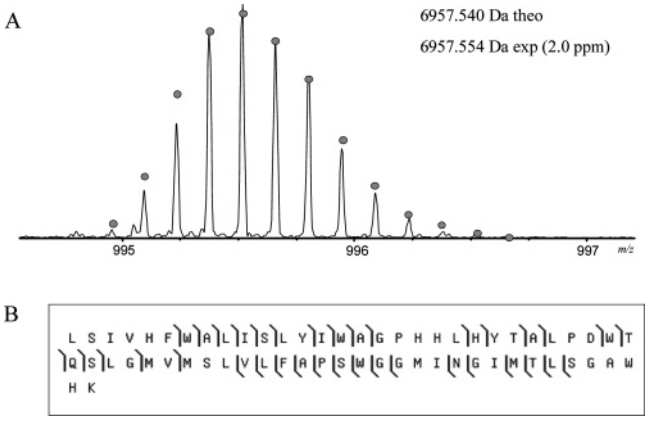

FIGURE 4: Mass spectrum and fragmentation of the tryptic L243−K304 peptide from the C-type oxygen reductase from *V. cholerae*. (A) Mass spectrum of the peptide. The circles show the theoretical isotope heights for a peptide of the given mass. (B) CAD MS/MS fragmentation results.

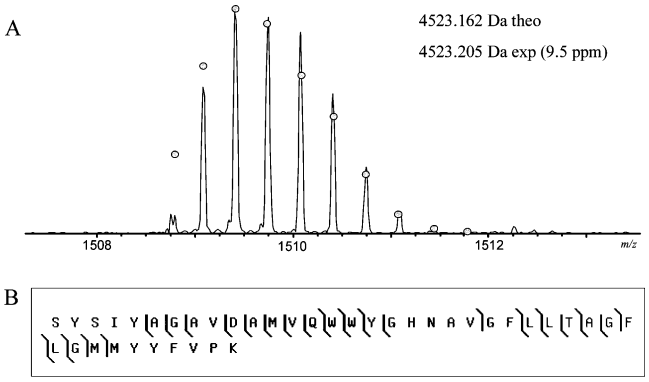

FIGURE 5: Mass spectrum and fragmentation of the tryptic S193−K232 peptide from the C-type oxygen reductase from *V. cholerae*. (A) Mass spectrum of the peptide. The circles show the theoretical isotope heights for a peptide of the given mass. (B) CAD MS/MS fragmentation results.

is between residues that are only four amino acids apart on the same transmembrane helix (H284−Y288 in the *R. sphaeroides* A-type oxygen reductase), whereas there are 44 amino acids between the cross-linked residues in the C-type oxygen reductases, which span two helices (H211−Y255 in the *V. cholerae* C-type oxygen reductase). The data show definitively that the cross-link is present between His284 and Tyr288 in subunit I of the *R. sphaeroides* A-type oxygen reductase, and no fragments with the molecular mass expected for the non-cross-linked peptide were detected

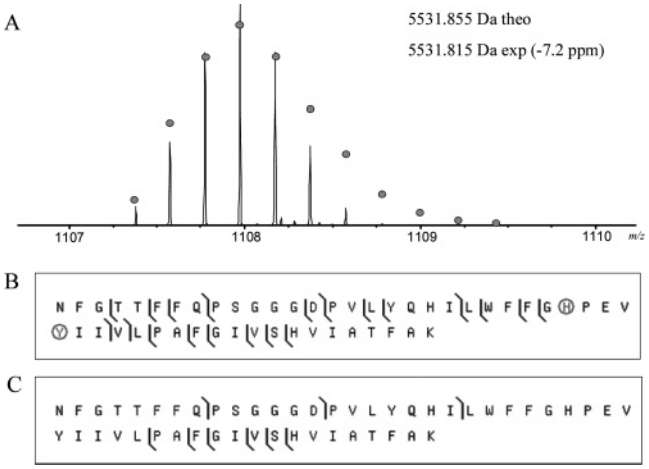

FIGURE 6: Mass spectrum and fragmentation of the cross-linked peptide from the A-type oxygen reductase from *R. sphaeroides*. (A) The mass spectrum of the cross-linked tryptic N258−K307 peptide. The circles show the theoretical isotope heights for a peptide of the given mass. The mass spectrum shows that only the cross-linked species is detected in the tryptic digest. (B) CAD MS/MS fragmentation results when analyzed with the cross-link present (the histidine and tyrosine are circled) and (C) without the cross-link. Multiple fragments containing the cross-link are detected, whereas no fragments lacking it are detected.

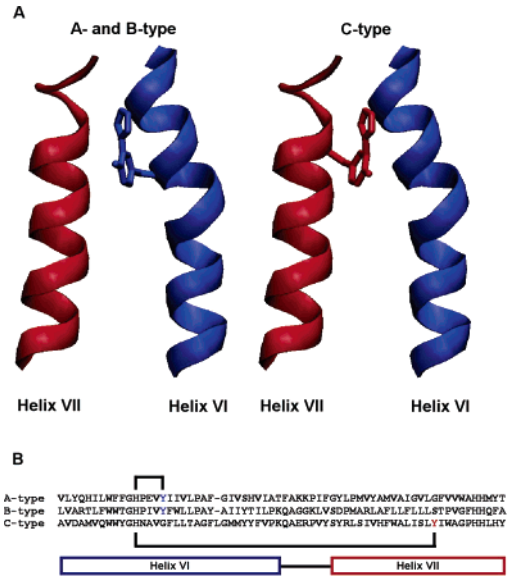

FIGURE 7: Novel cross-linked cofactor present in all three heme-copper oxygen reductase families. (A) The active-site tyrosine forming the cofactor originates from helix VI in the A- and B-type oxygen reductases, while in the C-type oxygen reductases, it originates from helix VII. This is the first example of the evolutionary migration of a post-translationally modified active-site residue. (B) The cross-link is formed between a histidine and tyrosine within helix VI in the A- and B-type oxygen reductases. In the C-type oxygen reductases the cross-link is formed between a histidine in helix VI and a tyrosine in helix VII, covalently coupling the helices together. This figure was generated using VMD (*45*).

(Figure 6). In agreement with the latest X-ray structure of the *R. sphaeroides* A-type oxygen reductase (S. Ferguson-Miller, personal communication), it is concluded that the His−Tyr cross-link is present in the entire population of this A-type oxygen reductase. At this time, it is unclear whether the occupancy of the cross-link in the C-type reductase is less than 100% in vivo or if the non-cross-linked peptides are an artifact of the sample preparation or mass spectrometry. Although the A-type reductase appears to be entirely cross-linked, the His−Tyr bond lability may be higher in the C-type under the analysis conditions.

DISCUSSION

Presence of an Active-Site Cross-Linked Cofactor in C-Type Heme-Copper Oxygen Reductases. This work demonstrates that a novel cross-linked cofactor is present in all three families of the heme-copper oxygen reductases (Figure 7). This verifies the prediction by molecular modeling (*10*, *11*) of the presence of an active-site tyrosine in the C-type oxygen reductases that is structurally and functionally equivalent to the active-site tyrosine in the A- and B-type oxygen reductases. It is also a unique structural feature which separates the oxygen reductases from other members of the heme-copper superfamily, notably NO reductases. The analysis of the C-type oxidase also revealed the presence of a population of the enzyme without the His−Tyr cross-link, but this is likely an artifact either of the conditions of the expression of the enzyme (e.g., incomplete incorporation of copper) or of the sample preparation. It is clear that collisionally activated fragmenation of the isolated cross-linked peptide during MS/MS analysis can result in scission of the cross-linking bond. However, the non-cross-linked peptide is also apparent in the absence of collisionally activated fragmentation in the mass spectrometer. This suggests that either the non-cross-linked enzyme is present within the trypsin digest or the cross-link in the C-type enzyme is more labile than that of the A-type enzyme either during the electropray process or in the trapping and cooling of the ions in the mass spectrometer. While the manuscript was being revised after initial review, Rauhamaki et al. (*21*) published a paper which demonstrates by MALDI mass spectrometry the presence of the His−Tyr cross-link in the C-type oxygen reductase from *R. sphaeroides*. The report by Rauhamaki et al. (*21*) does not indicate any non-cross-linked protein, so it is very likely that the cross-link is present in all properly assembled enzymes. It can be concluded from our work and that of Rauhamaki et al. (*21*) that the presence of the active-site His−Tyr cross-link is a universal feature of the C-type oxygen reductases and, by extension, all heme-copper oxygen reductases.

A Unified Catalytic Mechanism for All Oxygen Reductase Families. The novel cross-linked cofactor is thought to form as a result of the generation of a tyrosine radical in the active site, presumably upon the initial turnover of the reduced enzyme with O_2. Conceivably, this could be a side reaction and not essential for enzyme function. However, replacement of the active-site tyrosine with a phenylalanine in the *R. sphaeroides* A-type oxygen reductase not only resulted in an inactive enzyme but also altered the metal ligation in the active site (*22*). This suggests that the cross-link is needed to maintain the structure of the active site. Furthermore, work by Uchida et al. (*23*) demonstrated that substituting d^4-Tyr for tyrosine resulted in a large decrease in the enzymatic activity of an *Escherichia coli* A-type oxygen reductase, and the spectroscopic properties suggested that the His−Tyr cross-link was not formed. These observations suggest that the cross-link is not simply an irrelevant side product of the chemistry at the active site but is essential for the function of the heme-copper oxygen reductases. The active-site

tyrosine is proposed to donate both a proton and an electron to facilitate cleavage of the O−O bond (*6*−*8*, *24*−*26*). It is clear that an amino acid radical does form during the catalytic cycle of the oxygen reductase (*27*−*31*), and the active-site tyrosine is a logical primary electron donor for the chemistry. There is no evidence from rapid-quench electron paramagnetic resonance (EPR) spectroscopy for rapid formation of a tyrosine radical (*28*, *32*), but it would likely be EPR-silent due to the proximity of the metals at the active site. Attempts to demonstrate the presence of a radical by Fourier-transform infrared (FTIR) spectroscopy (*33*, *34*) and by iodination of the amino acid radical (*6*) have provided data consistent with the formation of neutral tyrosyl radical, but these data are acquired over a longer time period allowing for radical migration. Indeed, the strongest argument for the formation of a radical at the active-site tyrosine may be the fact that the His-Tyr cross-link is present. Presumably, the cross-link is a consequence of radical-based chemistry that occurs during the initial turnovers of the enzyme. The data strongly suggest that all heme-copper oxygen reductases utilize the same catalytic mechanism of hydrogen atom donation for oxygen bond scission.

Functional Role of the His−*Tyr Cross-Link.* The function of the cross-link has been the subject of considerable speculation as well as investigation. Recent studies with model compounds (*35*−*39*) as well as computational studies (*26*, *40*) have suggested a possible functional significance for the cross-link. The cross-linked histidine withdraws electrons from the tyrosine, resulting in a lower pK_a and a higher midpoint potential of the tyrosine (*41*). Conversely, the redox state and protonation state of the tyrosine influence the electron donating capacity of the imidazole as a metal ligand, thus controlling the preferred ligand geometry about Cu_B (*35*). It has also been suggested that, due to the presence of the cross-linked tyrosine, the histidine ligand to Cu_B might be labile and move away from the metal during turnover, playing a key role in the proton pump mechanism (*40*). These studies, in conjunction with the presence of the cross-linked cofactor in all oxygen reductase families, suggests that the cofactor may be a required component for proton pumping. Further work is necessary to elucidate its role.

Evolutionary Migration of the Post-Translationally Modified Tyrosine. The post-translational modification of active-site amino acid residues to form novel cofactors in situ has been observed in a number of redox active enzymes (*42*). Some cofactors are produced via chemical modification of amino acid side chains (e.g., oxidation, methylation, and hydroxylation), whereas other cofactors are formed by cross-linking two or more amino acids together. These post-translationally cross-linked active-site amino acids can be found in tyrosinase, hemocyanin, and catechol oxidase (Cys−His), catalase-peroxidase (Met−Tyr−Trp), galactose oxidase (Tyr−Cys), catalase (His−Tyr-αC), and the A- and B-type heme-copper oxygen reductases (His−Tyr) (see ref *42*). The evolutionary migration of amino acids within a protein family can be defined as the situation in which residues that have the same structural or functional role and which share the same spatial location derive from different positions within their respective protein sequences. Evolutionary migration has been reported for active-site residues (*43*, *44*), but this is the first report of a post-translationally modified active-site residue. The active-site tyrosine forming the cross-linked cofactor is located within a different transmembrane helix in the C-type oxygen reductases (helix VII) in comparison to that of the A-type and B-type oxygen reductases (helix VI). It is currently unknown which state (the tyrosine being located in helix VI or helix VII) is ancestral.

REFERENCES

1. Pereira, M. M., Santana, M., and Teixeira, M. (2001) A Novel Scenario for the Evoluation of Haem-copper Oxygen Reductases, *Biochim. Biophys. Acta 1505*, 185−208.
2. Garcia-Horsman, J. A., Barquera, B., Rumbley, J., Ma, J., and Gennis, R. B. (1994) The Superfamily of Heme-Copper Respiratory Oxidases, *J. Bacteriol. 176*, 5587−5600.
3. Ostermeier, C., Harrenga, A., Ermler, U., and Michel, H. (1997) Structure at 2.7 Å Resolution of the *Paracoccus denitrificans* Two-Subunit Cytochrome *c* Oxidase Complexed with an Antibody F_v Fragment, *Proc. Natl. Acad. Sci. U.S.A. 94*, 10547−10553.
4. Tsukihara, T., Aoyama, H., Yamashita, E., Takashi, T., Yamaguichi, H., Shinzawa-Itoh, K., Nakashima, R., Yaono, R., and Yoshikawa, S. (1996) The Whole Structure of the 13-Subunit Oxidized Cytochrome c Oxidase at 2.8 Å, *Science 272*, 1136−1144.
5. Soulimane, T., Buse, G., Bourenkov, G. P., Bartunik, H. D., Huber, R., and Than, M. E. (2000) Structure and Mechanism of the Aberrant ba_3-cytochrome c Oxidase from *Thermus thermophilus*, *EMBO J. 19*, 1766−1776.
6. Proshlyakov, D. A., Pressler, M. A., DeMaso, C., Leykam, J. F., DeWitt, D. L., and Babcock, G. T. (2000) Oxygen Activation and Reduction in Respiration: Involvement of Redox-Active Tyrosine 244, *Science 290*, 1588−1591.
7. Gennis, R. B. (1998) Multiple Proton-conducting Pathways in Cytochrome Oxidase and a Proposed Role for the Active-site Tyrosine, *Biochim. Biophys. Acta 1365*, 241−248.
8. Babcock, G. T. (1999) How Oxygen is Activated and Reduced in Respiration, *Proc. Natl. Acad. Sci. U.S.A. 96*, 12971−12973.
9. Buse, G., Soulimane, T., Dewor, M., Meyer, H. E., and Blüggel, M. (1999) Evidence for a Copper-coordinated Histidine-tyrosine Cross-link in the Active Site of Cytochrome Oxidase, *Protein Sci. 8*, 985−990.
10. Hemp, J., Christian, C., Barquera, B., Gennis, R. B., and Martinez, T. J. (2005) Helix Switching of a Key Active-Site Residue in the Cytochrome cbb_3 Oxidases, *Biochemistry 44*, 10766−10775.
11. Sharma, V., Puustinen, A., Wikstrom, M., and Laakkonen, L. (2006) Sequence analysis of the cbb3 oxidases and an atomic model for the *Rhodobacter sphaeroides* enzyme, *Biochemistry 45*, 5754−5765.
12. Wessel, D., and Flugge, U. I. (1984) A method for the quantitative recovery of protein in dilute solution in the presence of detergents and lipids, *Anal. Biochem. 138*, 141−143.
13. Whitelegge, J. P., le Coutre, J., Lee, J. C., Engel, C. K., Prive, G. G., Faull, K. F., and Kaback, H. R. (1999) Toward the bilayer proteome, electrospray ionization-mass spectrometry of large, intact transmembrane proteins, *Proc. Natl. Acad. Sci. U.S.A. 96*, 10695−10698.
14. Patrie, S. M., Charlebois, J. P., Whipple, D., Kelleher, N. L., Hendrickson, C. L., Quinn, J. P., Marshall, A. G., and Mukhopadhyay, B. (2004) Construction of a hybrid quadrupole/Fourier transform ion cyclotron resonance mass spectrometer for versatile MS/MS above 10 kDa, *J. Am. Soc. Mass Spectrom. 15*, 1099−1108.
15. Senko, M. W., Canterbury, J. D., Guan, S., and Marshall, A. G. (1996) A high-performance modular data system for Fourier transform ion cyclotron resonance mass spectrometry, *Rapid Commun. Mass Spectrom. 10*, 1839−1844.
16. Patrie, S. M., Ferguson, J. T., Robinson, D. E., Whipple, D., Rother, M., Metcalf, W. W., and Kelleher, N. L. (2006) Top down mass spectrometry of <60-kDa proteins from *Methanosarcina acetivorans* using quadrupole FRMS with automated octopole collisionally activated dissociation, *Mol. Cell. Proteomics 5*, 14−25.
17. Senko, M. W., Hendrickson, C. L., Emmett, M. R., Shi, D.-H., and Marshall, A. G. (1997) External Accumulation of Ions for Enhanced Electrospray Ionization Fourier Transform Ion cyclotron Resonance Mass Spectrometry, *J. Am. Soc. Mass Spectrom. 8*, 970−976.

18. Horn, D. M., Zubarev, R. A., and McLafferty, F. W. (2000) Automated reduction and interpretation of high resolution electrospray mass spectra of large molecules, *J. Am. Soc. Mass Spectrom. 11*, 320−332.
19. LeDuc, R. D., Taylor, G. K., Kim, Y. B., Januszyk, T. E., Bynum, L. H., Sola, J. V., Garavelli, J. S., and Kelleher, N. L. (2004) ProSight PTM: An integrated environment for protein identification and characterization by top-down mass spectrometry, *Nucleic Acids Res. 32*, W340−W345.
20. Roepstorff, P., and Fohlman, J. (1984) Proposal for a common nomenclature for sequence ions in mass spectra of peptides, *Biomed. Mass Spectrom. 11*, 601.
21. Rauhamaki, V., Baumann, M., Soliymani, R., Puustinen, A., and Wikstrom, M. (2006) Identification of a histidine-tyrosine cross-link in the active site of the cbb3-type cytochrome c oxidase from *Rhodobacter sphaeroides*, *Proc. Natl. Acad. Sci. U.S.A.* (in press).
22. Das, T. K., Pecoraro, C., Tomson, F. L., Gennis, R. B., and Rousseau, D. L. (1998) The Post-Translational Modification in Cytochrome *c* Oxidase Is Required To Establish a Functional Environment of the Catalytic Site, *Biochemistry 37*, 14471−14476.
23. Uchida, T., Mogi, T., Nakamura, H., and Kitagawa, T. (2004) Role of Tyr-288 at the dioxygen reduction site of cytochrome bo studied by stable isotope labeling and resonance raman spectroscopy, *J. Biol. Chem. 279*, 53613−53620.
24. Blomberg, M. R. A., Siegbahn, P. E. M., Babcock, G. T., and Wikström, M. (2000) O−O Bond Splitting Mechanism in Cytochrome Oxidase, *J. Inorg. Biochem. 80*, 261−269.
25. Blomberg, M. R., Siegbahn, P. E., and Wikström, M. (2003) Metal-bridging Mechanism for O−O Bond Cleavage in Cytochrome *c* Oxidase, *Inorg. Chem. 42*, 5231−5243
26. Bu, Y., and Cukier, R. I. (2005) Structural character and energetics of tyrosyl radical formation by electron/proton transfers of a covalently linked histidine-tyrosine: A model for cytochrome c oxidase, *J. Phys. Chem. B 109*, 22013−22026.
27. MacMillan, F., Kannt, A., Behr, J., Prisner, T., and Michel, H. (1999) Direct Evidence for Tyrosine Radical in the Reaction of Cytochrome *c* Oxidase with Hydrogen Peroxide, *Biochemistry 38*, 9179−9184.
28. Wiertz, F. G. M., Richter, O.-M. H., Cherepanov, A. V., MacMillan, F., Ludwig, B., and de Vries, S. (2004) An Oxoferryl Tryptophan Radical Catalytic Intermediate in Cytochrome *c* and Quinol Oxidasses Trapped by Microsecond Freeze-hyperquenching (MHQ), *FEBS Lett. 575*, 127−130.
29. MacMillan, F., Budiman, K., Angerer, H., and Michel, H. (2006) The Role of Tryptophan 272 in the *Paracoccus denitrificans* Cytochrome *c*, Oxidase, *FEBS Lett. 580*, 1345−1349.
30. Rich, P. R., Rigby, S. E. J., and Heathcote, P. (2002) Radicals associated with the Catalytic Intermediates of Bovine Cytochrome *c* Oxidase, *Biochim. Biophys. Acta 1554*, 137−146.
31. Budiman, K., Kannt, A., Lyubenova, S., Richter, O.-M. H., Ludwig, B., Michel, H., and MacMillan, F. (2004) Tyrosine 167: The Origin of the Radical Species Observed in the Reaction of Cytochrome *c* Oxidase with Hydrogen Peroxide in *Paracoccus denitrificans*, *Biochemistry 43*, 11709−11716.
32. Wiertz, F. G. M., and de Vries, S. (2006) Low-temperature Kinetic Measurements of Microsecond Freeze-hyperquench (MHQ) Cytochrome Oxidase Monitored by UV-Visible Spectroscopy with a Newly Designed Cuvette, *Biochem. Soc. Trans. 34*, 136−138.
33. Iwaki, M., Puustinen, A., Wikstrom, M., and Rich, P. R. (2004) ATR-FTIR spectroscopy and isotope labeling of the PM intermediate of *Paracoccus denitrificans* cytochrome c oxidase, *Biochemistry 43*, 14370−14378.
34. Nyquist, R. M., Heitbrink, D., Bolwien, C., Gennis, R. B., and Heberle, J. (2003) Direct Observation of Protonation Reactions During the Catalytic Cycle of Cytochrome *c* Oxidase, *Proc. Natl. Acad. Sci. U.S.A. 100*, 8715−8720.
35. Pesavento, R. P., Pratt, D. A., Jeffers, J., and van der Donk, W. A. (2006) Model studies of the Cu(B) site of cytochrome c oxidase utilizing a Zn(II) complex containing an imidazole-phenol cross-linked ligand, *Dalton Trans.*, 3326−3337
36. Pratt, D. A., Pesavento, R. P., and van der Donk, W. A. (2005) Model studies of the histidine-tyrosine cross-link in cytochrome *c* oxidase reveal the flexible substituent effect of the imidazole moiety, *Org. Lett. 7*, 2735−2738.
37. Kim, E., Kamaraj, K., Galliker, B., Rubie, N. D., Moenne-Loccoz, P., Kaderli, S., Zuberbuhler, A. D., and Karlin, K. D. (2005) Dioxygen reactivity of copper and heme-copper complexes possessing an imidazole-phenol cross-link, *Inorg. Chem. 44*, 1238−1247.
38. Tomson, F. L., Bailey, J. A., Gennis, R. B., Unkefer, C. J., Li, Z., Silks, L. A., Martinez, R. A., Donohoe, R. J., Dyer, R. B., and Woodruff, W. H. (2002) Direct Infrared Detection of the Covalently Ring-Linked His-Tyr Structure in the Active Site of the Heme-Copper Oxidases, *Biochemistry 41*, 14383−14390.
39. Cappuccio, J. A., Ayala, I., Elliott, G. I., Szundi, I., Lewis, J., Konopelski, J. P., Barry, B. A., and Einarsdóttir, Ó. (2002) Modeling the Active Site of Cytochrome Oxidase: Synthesis and Characterization of a Cross-linked Histidine-Phenol, *J. Am. Chem. Soc. 124*, 1750−1760.
40. Colbran, S. B., and Paddon-Row, M. N. (2003) Could the tyrosine-histidine ligand to CuB in cytochrome c oxidase be coordinatively labile? Implications from a quantum chemical model study of histidine substitutional lability and the effects of the covalent tyrosine-histidine cross-link, *J. Biol. Inorg. Chem. 8*, 855−865.
41. McCauley, K. M., Vrtis, J. M., Dupont, J., and van der Donk, W. A. (2000) Insights into the Functional Role of the Tyrosine-Histidine Linkage in Cytochrome *c* Oxidase, *J. Am. Chem. Soc. 122*, 2403−2404.
42. Okeley, N. M., and van der Donk, W. A. (2000) Novel cofactors via post-translational modifications of enzyme active sites, *Chem. Biol. 7*, R159−R171.
43. Todd, A. E., Orengo, C. A., and Thornton, J. M. (2002) Plasticity of enzyme active sites, *Trends Biochem. Sci. 27*, 419−426.
44. Hasson, M. S., Schlichting, I., Moulai, J., Taylor, K., Barrett, W., Kenyon, G. L., Babbitt, P. C., Gerlt, J. A., Petsko, G. A., and Ringe, D. (1998) Evolution of an enzyme active site: The structure of a new crystal form of muconate lactonizing enzyme compared with mandelate racemase and enolase, *Proc. Natl. Acad. Sci. U.S.A. 95*, 10396−10401.
45. Humphrey, W., Dalke, A., and Schulten, K. (1996) VMD: Visual Molecular Dynamics, *J. Mol. Graphics 14*, 33−38.
46. Taylor, G. K., Kim, Y. B., Forbes, A. J., Meng, F., McCarthy, R., and Kelleher, N. L. (2003) Web and database software for identification of intact proteins using "top down" mass spectrometry, *Anal. Chem. 75*, 4081−4086.

BI062026U